Available online at www.sciencedirect.com

SciVerse ScienceDirect

Ceramics International 38 (2012) 5453–5459

CERAMICS INTERNATIONAL

www.elsevier.com/locate/ceramint

Synthesis of $Lu_2Ti_2O_7$ nano-powders by salt modified sol–gel process

Bao-rang Li *, Hui Gao, Jun-peng Liu, Zhi-wei Yang

Key Laboratory of Condition Monitoring and Control or Power Plant Equipment, North China Electric Power University, Beijing 102206, China

Received 30 January 2012; received in revised form 23 March 2012; accepted 23 March 2012
Available online 7 April 2012

Abstract

Nano-sized $Lu_2Ti_2O_7$ powders have been prepared successfully by a chloride salt modified sol–gel process, by using tetrabutyl titanate and lutecium nitrate as precursors. The results indicate that salt precipitated during the synthesis process can form a thin layer of salt crust on the surface of the newly formed nano-particles and prevent re-agglomeration and hinder the particle growth resulting in well-dispersed $Lu_2Ti_2O_7$ nano-crystals. However, the increased salt contents can also lead to the significant size increase of the formed particles. Meanwhile, different types of salt species differently affect on the particle morphologies. Based on the above observation, well-dispersed spherical $Lu_2Ti_2O_7$ nano-crystals with an average particle size of about 50 nm can be obtained at 850 °C by the modified sol–gel process with precursor to NaCl ratio of 1:15.
© 2012 Elsevier Ltd and Techna Group S.r.l. All rights reserved.

Keywords: A. Powders: chemical preparation; A. Sol–gel processes; C. Thermal properties

1. Introduction

$A_{2+x}B_{2-x}O_{7-\delta}$ (A = Sm–Lu; B = Ti, Zr, Hf; x = 0–0.67) pyrochlores have attracted considerable attention because some of them are comparable in high-temperature oxygen ion conductivity to the well-known solid electrolytes ZrO_2–8–12 mol% Y_2O_3. Of particular interest are the $A_{2+x}Ti_{2-x}O_{7-\delta}$ (A = Er–Lu, x = 0–0.096) and $Ho_{2+x}Ti_{2-x}O_{7-\delta}$ (x = 0.48–0.67) pyrochlore-like titanates, which offer the highest oxygen ion conductivity in this family of materials, up to $\sim 1.4 \times 10^{-2}$ S/cm at 800 °C. Among these materials, $Lu_2Ti_2O_7$ with a pyrochlore structure can offer the highest ionic conductivity and is particularly suitable for application in an optical imaging system due to its high refractive index and high density [1,2]. Traditionally, $Lu_2Ti_2O_7$ is prepared by solid-state reaction [3,4], namely the metal oxides are used as precursors and the reaction reagents have to be sintered at higher temperature (>1100 °C) for a long time. Moreover, the products by solid-state reaction are usually non-uniform in part in chemical component and have large particle size, which is not favorable for their properties. Recently molten salt synthesis (MSS) method was employed successfully to synthesize the $Lu_2Ti_2O_7$ powders using TiO_2 and Lu_2O_3 as precursors. Especially two step calcinations technique was proved to be a novel method for fabrication of pure $Lu_2Ti_2O_7$ nano-particles [5,6]. In spite of this, one shortcoming of MSS is its multi-step washing for eliminating the salt. Moreover, different degrees of aggregation are usually presented in the final product. The solution-based soft chemical method is one of the typical strategies to synthesize nano-crystalline materials with perfect fine particles. Due to its unique features, a number of chemical methods have been used for synthesizing nano-powders, such as co-precipitation, the sol–gel method, hydrothermal synthesis, combustion and micro-wave-assisted synthesis [7–11]. Among these methods, sol–gel processing has gained an increasing importance in a variety of applications and has been the subject of intense study for last two decades. Sol–gel chemistry is an attractive alternative to other synthetic methods for many reasons. This method is low temperature, low cost, and can generally be done under room conditions with general lab equipment, all of which make processing convenient and inexpensive. So, based on the sol–gel process a large number of sophisticated materials have been prepared and studied and the corresponding theories elaborated. However, in all the cases discussed above the products obtained by sol–gel reaction had relatively large particle sizes caused by the high reaction temperatures. The molten salt-assisted chemical method of synthesizing nano-structured ceramic powders was recently employed [12–14]. It is based on the use of various inorganic salt additives (e.g. NaCl, KCl) as inert diluents to control the particle

* Corresponding author at: School of Energy, Power and Mechanical Engineering, North China Electric Power University, Beijing 102206, China.
E-mail address: libr@ncepu.edu.cn (B.-r. Li).

0272-8842/$36.00 © 2012 Elsevier Ltd and Techna Group S.r.l. All rights reserved.
http://dx.doi.org/10.1016/j.ceramint.2012.03.057

size. Alkali metal halide aids in transportation of the reactant species and prevents products grain growth by forming a protective layer around the particles. All these facilitate synthesis at low temperature, and positively affect the formation of fine grain products. To the best of our knowledge, there have been no prior reports of similar attempts to fabricate $Lu_2Ti_2O_7$ nano-powders up till the present. So, the emphasis of this work is to prepare and characterize well-dispersed $Lu_2Ti_2O_7$ nano-crystals synthesized via salt-assisted sol–gel method (SASG).

2. Experimental procedure

In the present study commercial tetrabutyl titanate, lutecium nitrate were used as the raw materials. All reagents were of analytical grade and used without further purification. Firstly, the deionized water was dropped into the mixture of lutecium nitrate and ethanol until lutecium nitrate was solved completely. Secondly, tetrabutyl titanate was dissolved in ethanol. The molar ratio of tetrabutyl titanate:lutecium nitrate is 1:1. The above two solutions were mixed together and the obtained solution was vigorously stirred for 15 h at 60 °C and further evaporated at 110 °C. Then, the as-prepared precursor was added to NaCl, ground for 20 min in an agate mortar. The ratio of the precursor to NaCl was chosen as 1:1, 1:5, 1:15, and 1:50. The mixture was then placed in a corundum crucible and annealed in a muffle furnace with heating rate of 10 °C/min. After heat treatment, the products were washed using hot deionized water to remove the residual salt. The products were then dried and characterized using an X-ray diffractometer (XRD, D/max-RB, Japan) for phase composition and a scanning electron microscopy (SEM, Model JSM-7401, Japan) for product morphology. Differential scanning calorimetry (DSC) measurements were made with the use of a liquid-nitrogen cooling accessory (DSC 404 F3 Pegasus).

3. Results and discussion

3.1. Sol–gel process

Fig. 1 illustrates the XRD patterns of $Lu_2Ti_2O_7$ nano-crystals calcined at 700–900 °C. It is easily found that Lu_2O_3, TiO_2 and $Lu_2Ti_2O_7$ coexist at 700 °C. TiO_2 tends to disappear gradually with temperature increasing. Almost no obvious TiO_2 can be detected at temperature higher than 750 °C. This indicates a large amount of $Lu_2Ti_2O_7$ phase can be synthesized at temperature higher than 700 °C by the sol–gel synthesis process.

With increasing of the calcinations temperature, the full width half-maximum (FWHM) decreases to some degree and the peaks become sharper. This implies that the calcinations temperature plays an important role on the control of the crystalline phase. When the sample is heated at 900 °C, all the intense diffraction peaks can be perfectly indexed to the cubic structure crystalline (JCPDS: 23-0375) indicating that the fluorite structure appears. In spite of these observations, the impure peaks, which are attributed to the residual Lu_2O_3, are still observed. This indicates that pure $Lu_2Ti_2O_7$ with fluorite structure cannot be synthesized by sol–gel method at

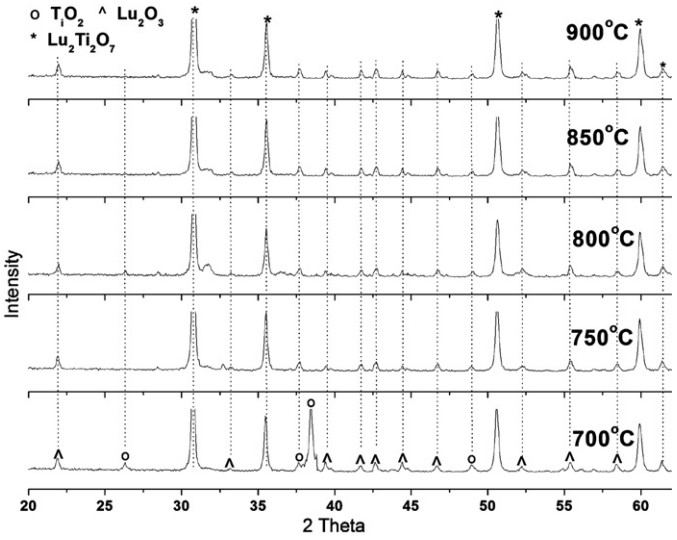

Fig. 1. XRD patterns of $Lu_2Ti_2O_7$ powders synthesized at various temperatures by sol–gel process without salt addition.

temperature lower than 900 °C. It was reported that conventional solid-state synthesis of pure $Lu_2Ti_2O_7$ phase was virtually impossible at a temperature < 1000 °C. Moreover, TiO_2 and Lu_2O_3 phase were reported to present with formation of $Lu_2Ti_2O_7$ [3,4]. When the molten salt route was applied to synthesize $Lu_2Ti_2O_7$, the similar results were obtained although two step calcinations technique (TSS) was reported to be a successful route for pure $Lu_2Ti_2O_7$ [5]. The similar results are also found in the sol–gel process.

In order to understand effects of the calcinations temperatures on the particle morphology, SEM micrographs of $Lu_2Ti_2O_7$ powders synthesized at different temperatures are shown in Fig. 2. When the calcinations temperature is as low as 750 °C, large blocks with pores and voids can be observed (Fig. 2(a)). The formed nano-particles agglomerate together and interconnect with each other forming a sponge-like mesostructure so that the average particle size cannot be distinguished very clearly. The presented pores and voids in the sponge-like mesostructure are probably due to the evolution of gases during synthesis reaction. With temperature increasing up to 800 °C, the pore size becomes enlarged obviously and at the same time the sponge-like mesostructure starts to disappear. The powders are mainly composed of sphere particles with an average size of about 30–40 nm at this temperature. Obvious change in the particles shape is observed when the temperature is increased to 850 °C, at which larger amounts of sphere particles start to be developed into ones with a relatively regular shape. Further increasing the calcinations temperature higher than 900 °C, no obvious change in particle morphology is found except the obvious duplex microstructure, as shown in Fig. 2(d), in which the small particles are less than 100 nm while the large particles size is increased to 300–400 nm.

3.2. Chloride salt modified sol–gel process

Fig. 3 shows the XRD patterns of the $Lu_2Ti_2O_7$ powders obtained through salt modified sol–gel process. The peaks to

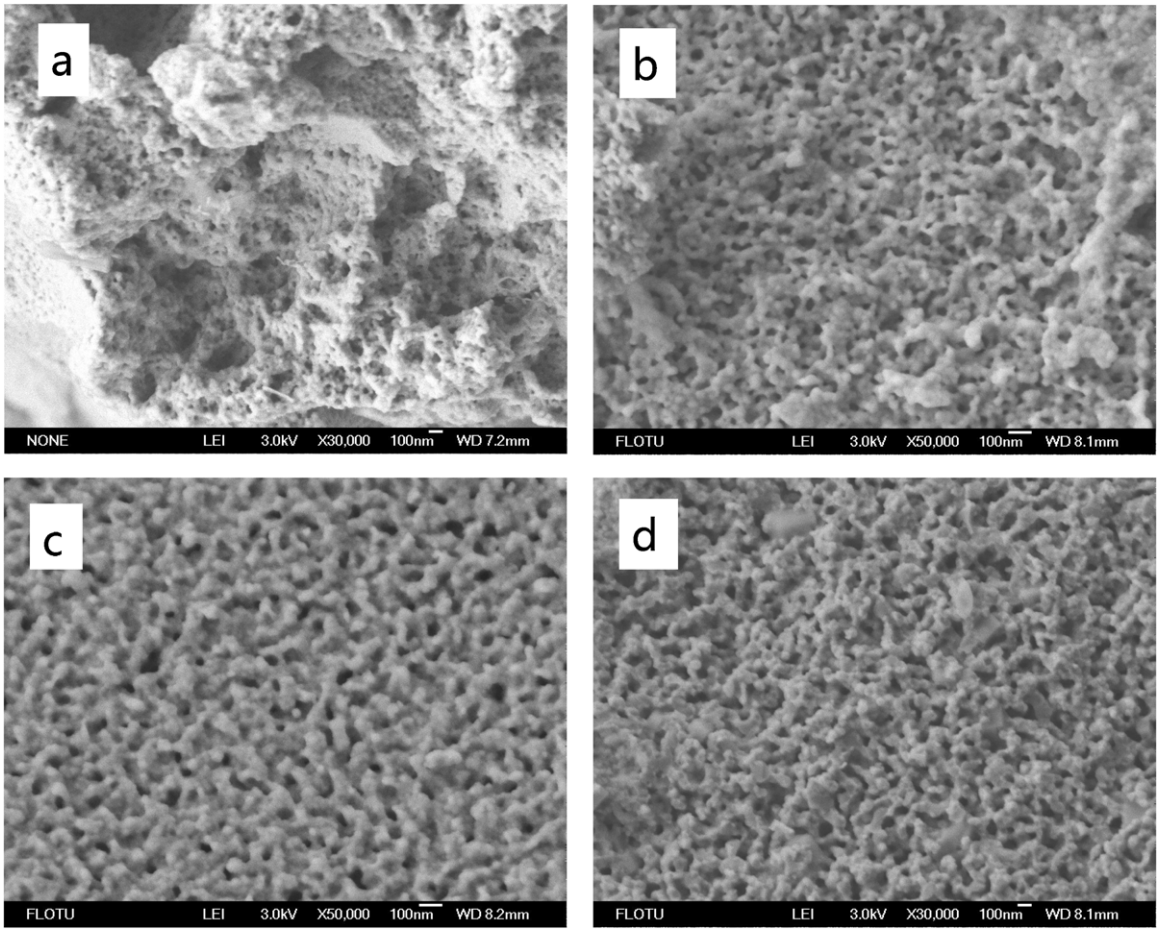

Fig. 2. Scanning electron micrographs of powders synthesized at different temperatures by sol–gel process without salt addition (a) 750/4 h; (b) 800/4 h; (c) 850/4 h; (d) 900/4 h.

which the arrows point are attributed to the residual Lu_2O_3 phase. KCl and NaCl are chosen as solvent, respectively. The precursor mixed with NaCl (Fig. 3(A)) is nearly fully converted to crystalline $Lu_2Ti_2O_7$ after being heated to 850 °C. In contrast, obvious secondary phase (mainly Lu_2O_3) can be found in the precursor mixed with KCl at the same temperature. This suggests NaCl is more effectively in favor of formation of pure $Lu_2Ti_2O_7$ phase than KCl.

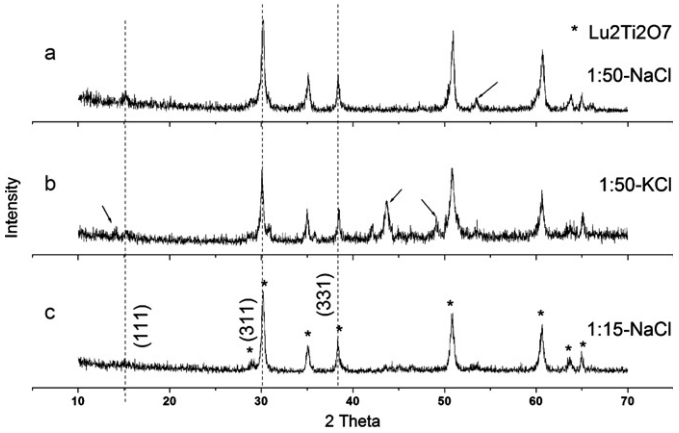

Fig. 3. XRD of $Lu_2Ti_2O_7$ powders synthesized from salt modified sol–gel process with different salt species calcined at 850 °C.

In order to reveal the influence of the salt contents upon $Lu_2Ti_2O_7$ powders formation, the mole ratios of the prepared reactant to salt are chosen from 1:1 to 1:50. NaCl is used as a solvent. The typical XRD patterns of $Lu_2Ti_2O_7$ powders synthesized under different conditions are also shown in Fig. 3. It is easily observed that in the case of NaCl, apart from the diffraction peaks of $Lu_2Ti_2O_7$ compound, additional peaks of the other phase are detected when the ratio of the prepared reactant to salt is equal to 1:50 (Fig. 3(A)). However, with decreasing the amount of salt, especially as the mole ratio is equal to 1:15 (Fig. 3(C)), the peaks of the secondary phase are found to disappear gradually. This phenomenon suggests that the salt contents play an important role in the development of $Lu_2Ti_2O_7$ particle crystallization. Especially, it is easily noted that the intensity of the pyrochlore super-lattice reflections (111, 311, 331 etc.) increase with salt addition by making comparison between Figs. 1 and 3. This indicates $Lu_2Ti_2O_7$ powders synthesized from SASG should have a pyrochlore structure. It was reported that the fluorite phase exists at 600–740 °C and lower annealing temperature of 850 °C provide the synthesis of $Lu_2Ti_2O_7$ with a pyrochlore structure containing the antisite defects, which decrease with the increased temperature and was decreased to 6% at 1050 °C [16]. This is consistent to our XRD results shown in Fig. 3 although Fig. 1 implies no obvious fluorite–pyrochlore phase transformation

happens even when the temperature is raised to 900 °C under sol–gel process without salt addition.

For quantifying the ratio of the $Lu_2Ti_2O_7$ phase under different conditions, the following equation was used:

$$Lu_2Ti_2O_7 \text{ phase fraction } (\%) = \frac{\sum I_{LTO(hkl)}}{\sum I_{(hkl)}} \quad (1)$$

where $\sum I_{LTO(h\,k\,l)}$ are the intensities of the diffraction peaks of $Lu_2Ti_2O_7$. The calculated fractions of the $Lu_2Ti_2O_7$ phase and its related phase transformation rates as a function of calcinations temperatures are shown in Fig. 4. Fig. 4(a) suggests the SASG method has an advantage over the conventional method in fabrication of pure $Lu_2Ti_2O_7$ powders. Fig. 4(b) is the phase transition rate, which is calculated using the datum of Fig. 4(a). For molten salt synthesis (MSS) method, its curves first go up and then down and the highest transition rate (corresponding to the point O) is obtained at around 800 °C. However, no such point is found for the sol–gel process. For sol–gel process, the phase transition rate is found to increase with temperature increasing although this trend can be modified by salt addition.

The MSS mechanism is a two step process consisting of nucleation and subsequent coarsening. The nucleation process has close relations to the solubility of the starting materials in the molten salt. For a simple two reactant system, two different cases can be distinguished: either both reactants are equally soluble in the molten salt or one oxide is more soluble than the other. In our studied system ($TiO_2 + Lu_2O_3$), it is the latter situation because TiO_2 was reported not to be soluble in molten alkali chlorides [6]. Lu_2O_3 dissolved in the salt and diffused to TiO_2. At the surface, it reacted in situ to synthesize $Lu_2Ti_2O_7$. TiO_2 acts as nucleated templates during the synthesis process. So MSS process is a typical inhomogeneous nucleation process. An explosive nucleation due to the presence of large amounts of TiO_2 templates can lead to the highest phase transition rate shown in Fig. 4(b). However, the sol–gel synthesis process is a homogeneous nucleation process because no such templates can be found for nucleation. So its phase transition rate increases gradually with temperature increasing.

In order to understand the effects of salt contents on the particle morphology, SEM micrographs of $Lu_2Ti_2O_7$ powders synthesized 850 °C under different conditions are shown in Fig. 5. From Fig. 5(c), we can see that the introduction of inert chloride salt into the sol–gel synthesis process breaks up the network structure of agglomerated nano-crystallites and well-dispersed nano-crystals are formed. The particles shown in Fig. 5(c) have spherical morphology and are mainly composed of regularly small particles with an average particle size of less than 50 nm. Moreover, by comparison Fig. 5(a) with Fig. 5(b), no obvious increment of the particle size can be observed in spite of the increased temperature. This indicates the salt addition is in a favor of controlling the abnormal particle growth. On the other hand, the $Lu_2Ti_2O_7$ particle size shows a strong dependence on the salt amounts. Fig. 5(e) implies the particle size become obviously large when the ratio of the prepared reactant to salt is decreased to 1:50. Another phenomenon observed in Fig. 5 is that the $Lu_2Ti_2O_7$ nano-crystals obtained by NaCl-assisted sol–gel process have more uniform particle size distribution and better dispersibility than that prepared by KCl-assisted sol–gel process. Fig. 5(d) suggests KCl tends to make the particles grow along one-dimensioned direction and finally formed in worm-like shape.

Fig. 6(a) shows the dependence of the particle sizes upon the calcinations temperature. The particle size was calculated using the Scherrer equation and further confirmed by SEM. Fig. 6(b) shows the dependence of the particle sizes upon the contents of salt. When the ratio of the precursor to NaCl is below 1:15, no obvious changes in particle size can be found. However, when the ratio of the precursor to NaCl is higher than 1:15, the curve becomes obviously sharp indicating quickly increasing of the particle size. The similar trend is also found in the relations between the calcinations temperature and particle size with no salt addition (Fig. 6(a)). No obvious change in particles size is found at temperatures below 800 °C. However, Fig. 6(a) indicates the increment of particle size with increased temperatures can be refrained significantly by adding NaCl.

The particles growth rate can be expressed by the following equation:

$$u = Dv_o\left[\exp\left(-\frac{Q}{kT}\right)\right] \quad (2)$$

where D is the particle diameter, v_o is the atomic jump frequency, Q is the activation energy for an atom to leave

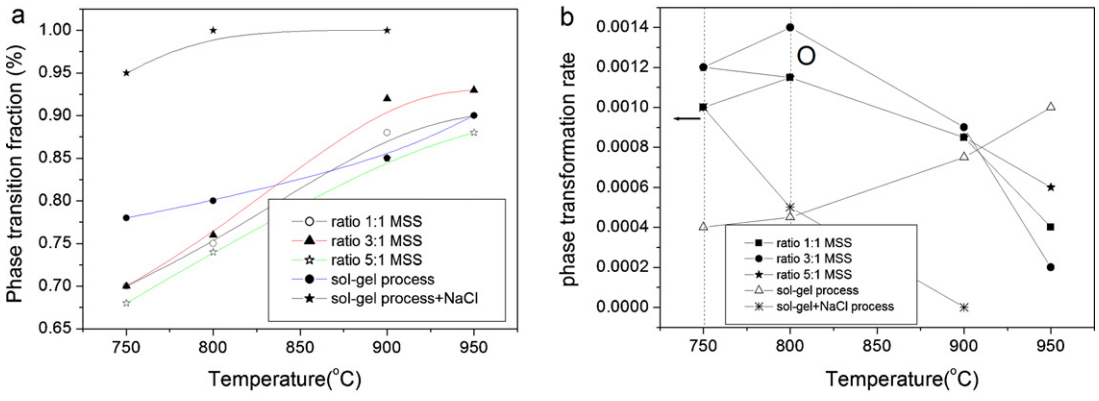

Fig. 4. (a) The temperature dependence of the phase transformation fraction; (b) the temperature dependence of the phase transition rate.

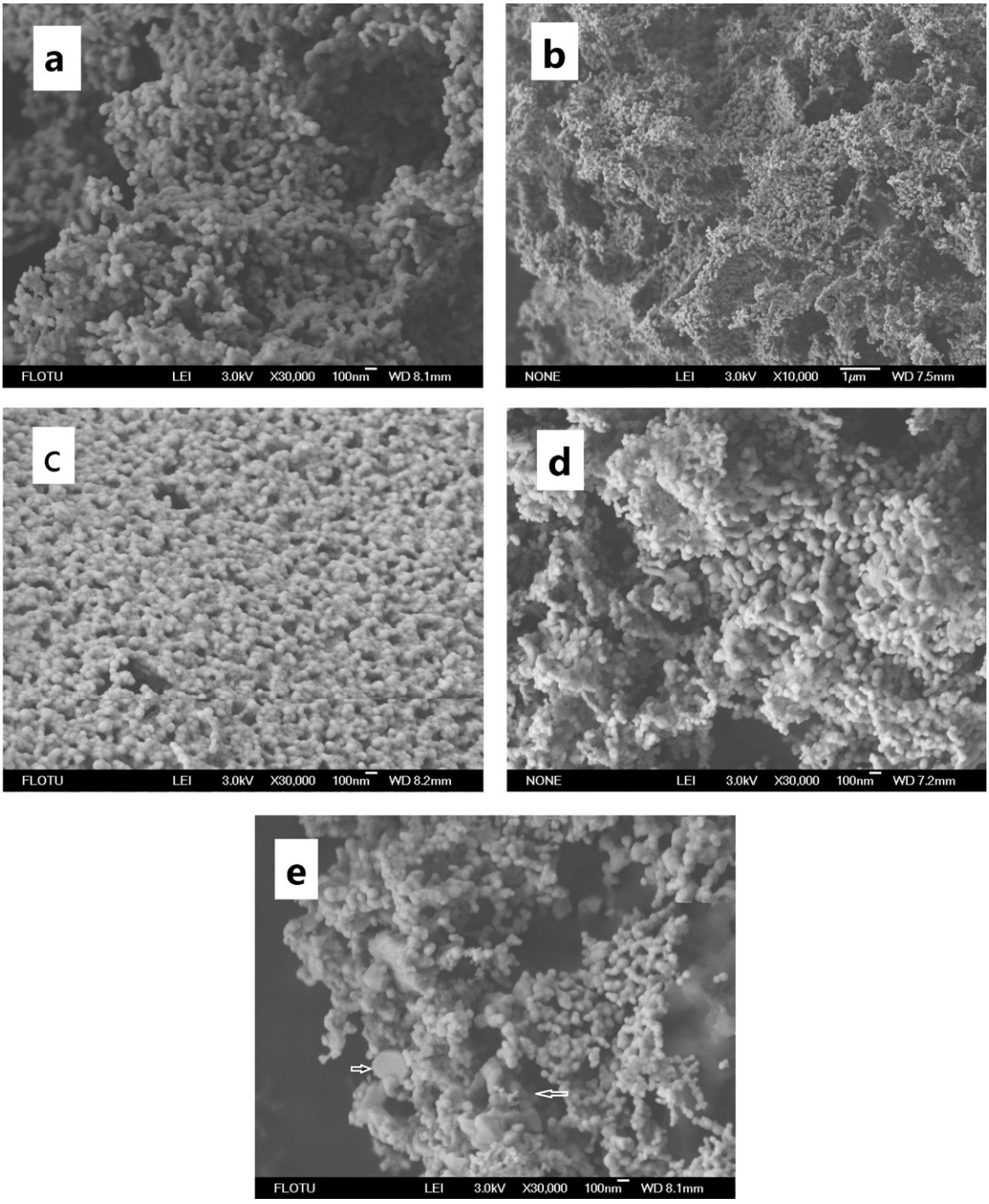

Fig. 5. Scanning electron micrographs of powders synthesized under different conditions (a) NCl, the ratio of the precursor to NaCl is 1:15, 850 °C; (b) NCl, the ratio of the precursor to NaCl is 1:15, 950 °C; (c) NCl, the ratio of the precursor to NaCl is 1:1, 850 °C; (d) KCl, the ratio of the precursor to KCl is 1:15, 850 °C; (e) NCl, the ratio of the precursor to NaCl is 1:50, 850 °C.

the matrix and attach itself to the growing phase, k is the gas constant and T is the calcinations temperature in Kelvin. Eq. (1) indicates the particle growth rate has close relations with the activation energy. The Arrhenius dependence of $Lu_2Ti_2O_7$ particles on the formation temperatures is depicted in Fig. 6(c). The activation energy for particle growth can be calculated from the plot of ln D vs. $1/T$. So the slopes of the dashed line indicate the average activation energies for particles growth.

It is easily found from Fig. 6(c) there are two distinct regions for no salt addition while no big difference in activation energy is found for NaCl-added sol–gel process. Sudden change in the activation energy implies that the synthesis process might experience a transition from a diffusion control mechanism to an interfacial reaction controlled mechanism, which can lead to a fast growth rate [15]. So the growth process of $Lu_2Ti_2O_7$ in which no any salt was added might undergo a possible transition when the temperature is increased higher than

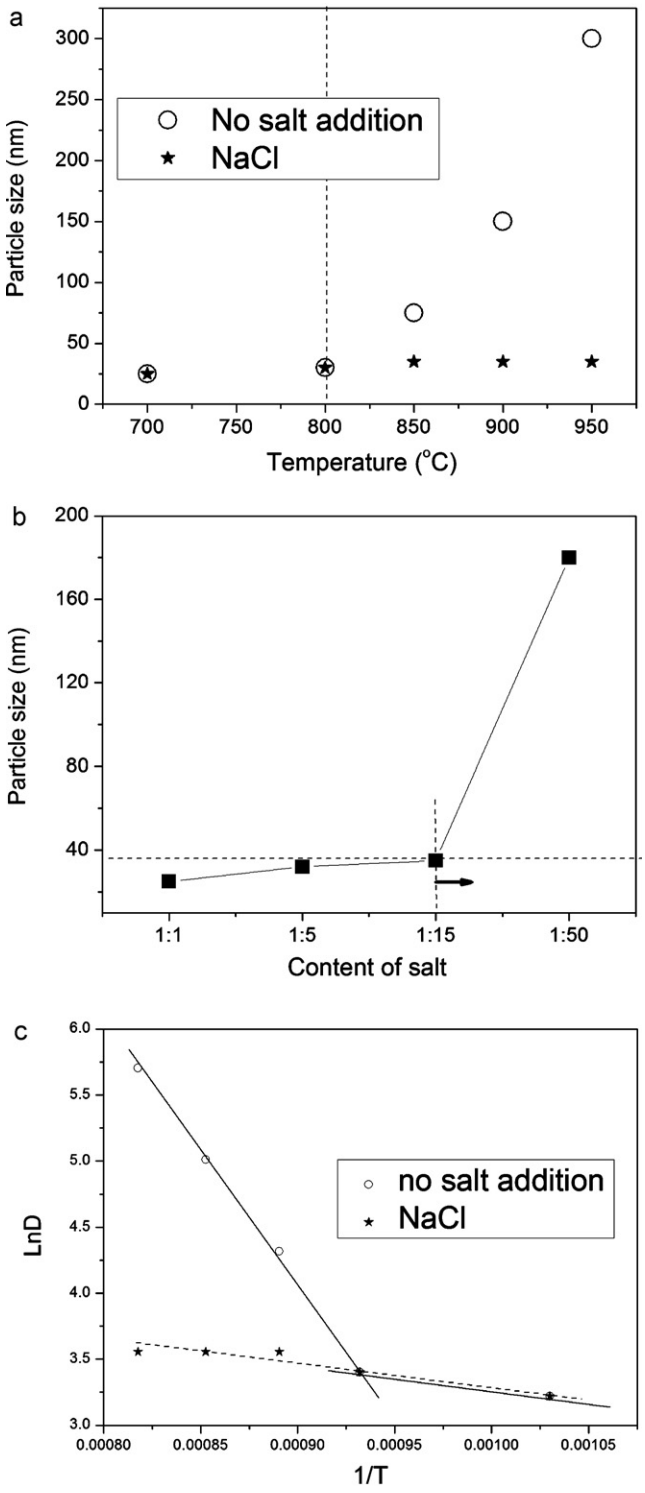

Fig. 6. (a) Dependence of $Lu_2Ti_2O_7$ particle size on the calcinations temperature; (b) dependence of $Lu_2Ti_2O_7$ particle size on the calcinations temperature salt content; (c) plots of 2 ln D (D: the average particle size) vs. $1/T$. The ratio of the precursor to NaCl is 1:15.

800 °C. When the $Lu_2Ti_2O_7$ powders is prepared by the sol–gel method, observations on SEM pictures disclose that the formed nano-particles interconnect with each other to form a sponge-like mesostructure at low temperature (Fig. 2(a)) and these formed small particles tend to contact and merge with each other resulting in large particles formation with the help of particle growth mechanism transition as the temperature is raised up to 850 °C. In the salt-modified sol–gel process, the salt precipitation in situ is completed instantly and can form a thin layer of salt crust on the surface of the newly formed nano-particles. After the rapid cooling, the salt-coated $Lu_2Ti_2O_7$ particles are trapped in the salt matrix, which can prevent the re-agglomeration. So the above referred particle growth mechanism transition is hindered effectively and the well-dispersed $Lu_2Ti_2O_7$ nano-crystals can be obtained. However, the effect of salt on the synthesis of $Lu_2Ti_2O_7$ would become dominated if the mole ratio of the precursors to salt is increased beyond the critical point, which is 1:15 in our studies. Under this case, the particle size of the $Lu_2Ti_2O_7$ powder would show a strong dependence on the salt contents. The particles size increases with the increased salt contents. This can be ascribed to the increases in the formation rate and the particle growth space with salt contents increasing because the increased salt contents might change either the melt viscosity or the solution of the oxides in the melt.

3.3. Thermal properties

Fig. 7 gives differential scanning calorimetry data recorded for $Lu_2Ti_2O_7$ poly-crystals. An obvious endo-thermal peak can be found in Fig. 7(a). It was reported that $Lu_2Ti_2O_7$ underwent reversible low-temperature (800–1200 °C) and high-temperature (above 1615 °C) order–disorder phase transition accompanied changes in structural order [16]. So, the endo-thermal peak near 1000 °C shown in Fig. 7(a) is attributable to the first fluorite to pyrochlore phase transformation. This temperature is about 150 °C higher than the results reported in Ref. [16]. That is to say, the transformation tends to shift to higher temperature significantly in our studies. Many factors such as doping, non-stoichiometry and synthesis procedure may influence defect structure and, accordingly, order–disorder transformation and properties. On the other hand, the transformation is also regarded to be connected to the complex stress conditions within the grains of polycrystalline $Lu_2Ti_2O_7$. The microstructure-constrained transformation strain energies and possible stress-relieving mechanisms contribute to the enhanced stability for fluorite phase.

The broadened and multistep thermal anomaly is noted in Fig. 7(b). This indicates no intense low-temperature phase transition at 800–1200 °C happens in the $Lu_2Ti_2O_7$ particles prepared by salt modified sol–gel process, which is corresponding to our XRD observations shown in Fig. 3. However, just as discussed previously, the pyrochlore structure derived from low temperature phase transformation is usually imperfect because of containing cation and anion defects, which can be eliminated gradually by increasing calcinations temperature higher than 1050 °C. So it is possible that the obtained pyrochlore structure in Fig. 3 should contain large amounts of defects. The broad and weak feature of DSC curve shown in Fig. 7(b) should have close relations to the defects recombination.

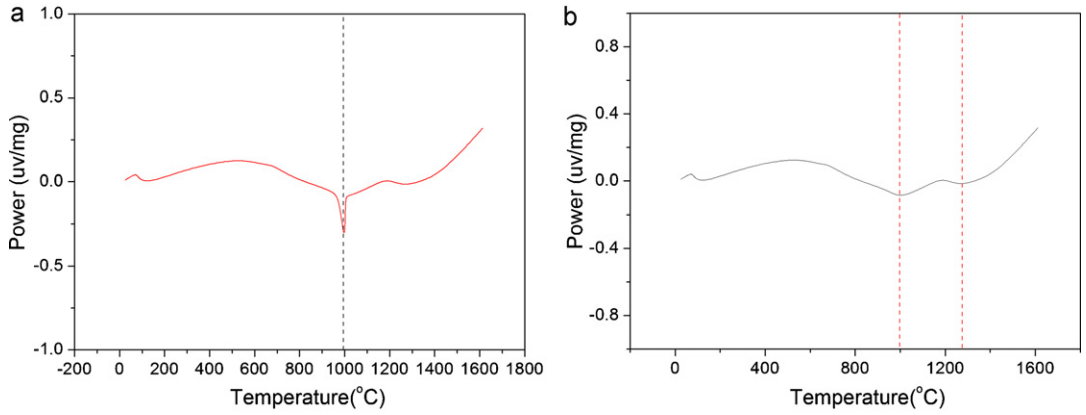

Fig. 7. DSC data for polycrystals, illustrating the dependence of phase transition thermal characteristics on the particle size (a) pure sol–gel process; (b) sol–gel process with NaCl addition.

4. Conclusions

The well-dispersed $Lu_2Ti_2O_7$ nano-crystals were successfully prepared by a chloride salt modified sol–gel process and the influences of chloride salt on the morphology characteristics of powders were evaluated in this paper. The results showed that the preparation temperature was lower and the product purity was largely improved by sol–gel process, compared with transitional solid-state method. Moreover, the calcinations temperature affects the particle sizes and morphology. The results also indicated that the introduction of inert chloride salt into the sol–gel synthesis process broke up the network structure of agglomerated nano-crystallites and resulted in the formation of well-dispersed nano-crystals. However, the crystallization and morphology of $Lu_2Ti_2O_7$ powders were affected greatly by the salt amounts and types. When the ratio of the precursor to NaCl was chosen as low as 1:15, the well-defined spherical $Lu_2Ti_2O_7$ powders with the particle size less than 50 nm were successfully synthesized at 850 °C by salt-assisted sol–gel method. The procedure reported here is simple and well-controlled for the synthesis of $Lu_2Ti_2O_7$ nano-crystals, and can be potentially applied to the preparation of other pyrochlore oxides.

References

[1] A.V. Shlyakhtina, L.G. Shcherbakova, A.V. Knotko, Studies of new order–disorder structural transitions in $Ln_2M_2O_7$ (Ln = Lu, Gd; M = Ti), Ferroelectrics 294 (2003) 175–190.

[2] A.V. Shlyakhtina, L.G. Shcherbakova, A.V. Knotko, A.V. Steblevskii, Study of the fluorite–pyrochlore–fluorite phase transitions in $Ln_2Ti_2O_7$ (Ln = Lu, Yb, Tm), Journal of Solid State Electrochemistry 8 (2003) 661–667.

[3] L. An, A. Ito, T. Goto, Fabrication of transparent lutetium oxide by spark plasma sintering, Journal of the American Ceramic Society 94 (2011) 695–698.

[4] L. An, A. Ito, T. Goto, Highly transparent lutetium titanium oxide produced by spark plasma sintering, Journal of the European Ceramic Society 31 (2011) 237–240.

[5] B.R. Li, N.Q. Zhang, H.B. Chang, D.Y. Liu, Preparation of $Lu_2Ti_2O_9$ nanopowders from oxides by molten salt method, Materials Letters 66 (2012) 39–41.

[6] B.R. Li, H.B. Chang, D.Y. Liu, X.N. Yuan, Synthesis of $Lu_2Ti_2O_7$ powders by molten salt method, Materials Chemistry and Physics 130 (2011) 755–759.

[7] Y. Xu, C. Wang, K.C. Tam, L. Li, Salt-assisted and salt-suppressed sol–gel transitions of methylcellulose in water, Langmuir 20 (2004) 646–652.

[8] V. Santagada, F. Frecentese, E. Perissutti, F. Fiorino, B. Severino, G. Caliendo, Microwave assisted synthesis: a new technology in drug discovery, Mini-Reviews in Medicinal Chemistry 9 (2009) 340–358.

[9] B. Liu, H.C. Zeng, Hydrothermal synthesis of ZnO nano-rods in the diameter regime of 50 nm, Journal of the American Chemical Society 125 (2003) 4430–4431.

[10] T. Mokkelbost, I. Kaus, T. Grande, M.-A. Einarsrud, Combustion synthesis and characterization of nano-crystalline CeO_2-based powders, Chemistry of Materials 16 (2004) 5489–5494.

[11] T.H. Cho, S.M. Park, M. Yoshio, T. Hirai, Y. Hideshima, Effect of synthesis condition on the structural and electrochemical properties of Li[Ni1/3Mn1/3Co1/3]O2 prepared by carbonate co-precipitation method, Journal of Power Sources 142 (2005) 306–312.

[12] Y. Huang, H.-q. Ye, W.-d. Zhuang, Y.-s. Hu, C.-l. Zhao, C. Li, S.-x. Guo, Preparation of Y_2O_3:Eu^{3+} phosphor by molten salt assisted method, Transactions of Nonferrous Metals Society of China 17 (2007) 644–648.

[13] B. Xia, I.W. Lenggoro, K. Okuyama, Synthesis of CeO_2 nano-particles by salt-assisted ultrasonic aerosol decomposition, Journal of Materials Chemistry 11 (2001) 2925–2927.

[14] H. Jiao, L. Wei, N. Zhang, M. Zhong, X. Jing, Melting salt assisted sol–gel synthesis of blue phosphor Y_2SiO_5:Ce, Journal of the European Ceramic Society 27 (2007) 185–189.

[15] B.-r. Li, X.-t. Liu, P.-l. Chen, Y.-s. Zheng, Effect of salt species on characterization of Bi_3NbTiO_9 powders prepared by molten salt method, Ceramics International 38 (2012) 105–110.

[16] A.V. Shlyakhtina, L.G. Shcherbakova, A.V. Knotko, A.V. Steblevskii, Study of the fluorite–pyrochlore–fluorite phase transitions in $Ln_2Ti_2O_7$ (Ln = Lu, Yb, Tm), Solid State Ionics 8 (2004) 661–667.